Water Air Soil Pollut (2023) 234:376
https://doi.org/10.1007/s11270-023-06386-6

Properties Controlling Phosphorus Adsorption and Stability in Amazonian Agro-Industrial Waste Biochars: a Multivariate Approach

Kleve Freddy Ferreira Canteral · Yan Nunes Dias · Antonio Rodrigues Fernandes

Received: 24 February 2023 / Accepted: 23 May 2023 / Published online: 5 June 2023

Abstract The application of biochar from agro-industrial residues of the Amazon is a key strategy to optimize the use of phosphorus (P) in agriculture and provide the proper management of these materials. In this study, we investigated the relationship between the chemical constituents of biochars from açaí seeds (BA), Brazil nut shells (BN) and palm kernel cake (BK) with phosphorus adsorption to identify the main properties that control this process and the thermochemical stability of carbon (C). Biochars were produced under slow pyrolysis (3.33 ºC min^{-1}) at 700 ºC and evaluated regarding their physicochemical properties, elemental composition and maximum P adsorption capacity (q_m). The interrelationship between the properties of the biochars was described by multivariate techniques: factor analysis (FA), canonical correlation analysis (CCA) and hierarchical cluster analysis. The multivariate approach allowed the analysis of the properties of biochars associated with q_m and provided the differentiation between the biochars derived from different agro-industrial residues. FA and CCA indicated a high association ($r \geq 0.93$; $p < 0.05$) of q_m with ash content, cation exchange capacity (CEC) and nitrogen (N) content. Therefore, small increments in these attributes can cause variation in the rate of P adsorption. The heatmap allowed the identification of greater similarities between BA and BN; and greater contrast between q_m with the aromaticity indices H/C and O/C and the polarity index (O + N)/C. Our results indicate that these biochars have the potential to adsorb P, increase the thermochemical stability of C in soil and represent a sustainable alternative for waste management of eastern Amazon.

Highlights
- Multivariate analysis identified the properties highly associated with q_m.
- The biochars showed high association between q_m and the properties ash, CEC and N.
- The woody biomasses BA and BN showed higher similarities between them.
- BA and BN are more recalcitrant than BK.
- C, H/C and O/C can be used as predictors of biochar chemical stability.

Supplementary Information The online version contains supplementary material available at https://doi.org/10.1007/s11270-023-06386-6.

K. F. F. Canteral (✉)
Department Engineering and Exact Sciences, School of Agricultural and Veterinarian Sciences, São Paulo State University (FCAV/UNESP), Via de Acesso Prof. Paulo Donato Castellane s/n, Jaboticabal, São Paulo 14884-900, Brazil
e-mail: canteralkleve@gmail.com

Y. N. Dias
Sustainable Development, Vale Institute of Technology, Belém, PA 66077-530, Brazil
e-mail: yanynd1@gmail.com

A. R. Fernandes
Institute of Agricultural Sciences, UFRA, Federal Rural University of the Amazon, Belém, Pará 66077-530, Brazil
e-mail: antonio.fernandes.ufra@gmail.com

Keywords Phosphorus recovery · Carbon stability · Waste disposal · Environmental contamination · Multivariate techniques

1 Introduction

Phosphorus (P) is a macronutrient for plants and its deficiency is one of the main limiting factors for crop growth and development, as most arable agricultural lands is P deficient (Arbelaez Breton et al., 2021). Globally, approximately 15 million tons of phosphate fertilizers are applied to agricultural lands each year in order to meet food demand (Zhang et al., 2016). Phosphorus is mainly extracted from phosphate rock reserves, which are non-renewable resources, which can be depleted due to increase in demand by crops and losses through erosion and fixation (Reitzel et al., 2019). On the other hand, continuous P fertilization and its accumulation in arable soils can result in large losses due to surface runoff, triggering changes in the P cycle in ecological systems, such as eutrophication of water bodies (Tan et al., 2022), with increased algal and phytoplankton blooms and reduced dissolved oxygen content in the environment (Xu et al., 2019). For these reasons, the development of green technologies that ensure environmental sustainability has been increasingly encouraged (Fahmy et al., 2020), reducing fixation and contamination from P loss, as well as the use of this non-renewable resource.

Alternative technologies that can be a source of P and release this element into the soil with greater utilization by crops have been employed, specifically biochar, as it is an effective and inexpensive material from renewable sources (Fahmy et al., 2020). Biochar is a stable and carbon-rich product formed by the thermal decomposition of biomasses such as agricultural and industrial residues under limited oxygen conditions (Lehmann & Joseph, 2009). The adsorption capacity of biochar depends on its physicochemical properties, such as pH (Xu et al., 2022; Zhou et al., 2017), and cation exchange capacity (Li et al., 2017). In turn, the properties of biochars are mainly dependent on the type of source material and pyrolysis conditions (Yu et al., 2017; Zhang et al., 2021). Recent studies have reported the positive effects of biochar on chemical, physical and biological properties of soils (Zhang et al., 2021), pollutant removal (Dai et al., 2020) and potential for carbon sequestration (Colantoni et al., 2016).

Recently, the special report on 1.5 °C global warming published by the Intergovernmental Panel on Climate Change (IPCC, 2018) included biochar as a promising negative emissions technology (NET), with potential estimated at 0.7 Gt Ceq year^{-1} (along with carbon sequestration). From this perspective, biochar is a potential method for C sequestration and greenhouse gas (GHG) emission mitigation, as it enables atmospheric CO_2 fixation via biomass photosynthesis that results in a stable and carbon-rich product after thermochemical treatment (Colantoni et al., 2016). Studies report that biochar production under slow pyrolysis conditions (lower heating rates and longer residence time) and high temperatures ($\geq$700 °C) tend to produce an alkaline material, with high ash contents, recalcitrant carbon, and low O/C and H/C ratios (Sato et al., 2019; Chatterjee et al., 2020), which are decisive factors for the potential for negative emissions. Such characteristics favor the adsorption of nutrients, such as P (Ghodszad et al., 2022; Schneider & Haderlein, 2016).

In the Brazilian Amazon, the productive chain of açaí fruit (*Euterpe oleracea* Mart.), Brazil nut (*Bertholletia excelsa* H.B.K) and palm oil (*Elaeis guineensis*) has high economic representation. The high national and international demand for processing these products has positively affected the region's economy, especially in the state of Pará, which contributes approximately 90% of the national production of these crops (IBGE, 2019; ABRAPALMA, 2019). However, residues from the processing of these fruits are usually discarded and accumulated irregularly in urban fairs, sewage systems and rivers in the region, compromising the health of the population, due to environmental contamination and proliferation of pathogenic organisms. Thus, the production of biochar from residues of açaí seeds (BA), Brazil nut shells (BN) and palm kernel cake (BK) can be a viable alternative to ensure the sustainable development of the Amazon, because in addition to solving agro-industrial waste management, it could be applied to remediate environments with high levels of P and increase the thermochemical stability of C in soils.

Despite the growing evidence on the importance of reusing agro-industrial residues as an ecological alternative for agronomic or environmental purposes, there are no studies that evaluated the use of

biochar from açaí, Brazil nuts and palm kernel cake for the adsorption of P and evaluated the stability of C in these materials, especially with multivariate data techniques. The multivariate approach can help to more efficiently explore the associations between these variables and simultaneously assess which of them contribute most to the process of P adsorption and C stability in biochars.

The hypothesis of this study is that the production of biochar at high temperature leads to a material with greater C content and stability, in addition to a greater potential for P adsorption. Thus, the objective of this work was to investigate the relationship between the chemical constituents of biochars from açaí seeds (BA), Brazil nut shells (BN) and palm kernel cake (BK) with phosphorus adsorption to identify the main properties that control this process and the thermochemical stability of C.

2 Material and Methods

2.1 Raw Materials

Residues of açaí (*Euterpe oleracea*) seeds and Brazil nut (*Bertholletia excelsa*) shells were collected in urban markets in the metropolitan region of Belém, and palm kernel cake, a by-product of oil palm (*Elaeis guineensis*) processing, was obtained from processing companies in the state of Pará, Brazil. These residues are widely produced in the Amazon and their disposal usually occurs in an irregular and inadequate manner (Fig. 1).

2.2 Preparation and Characterization of the Biochars

The samples of the collected residues were washed with deionized water and dried in an oven at 50 ºC for 24 h.

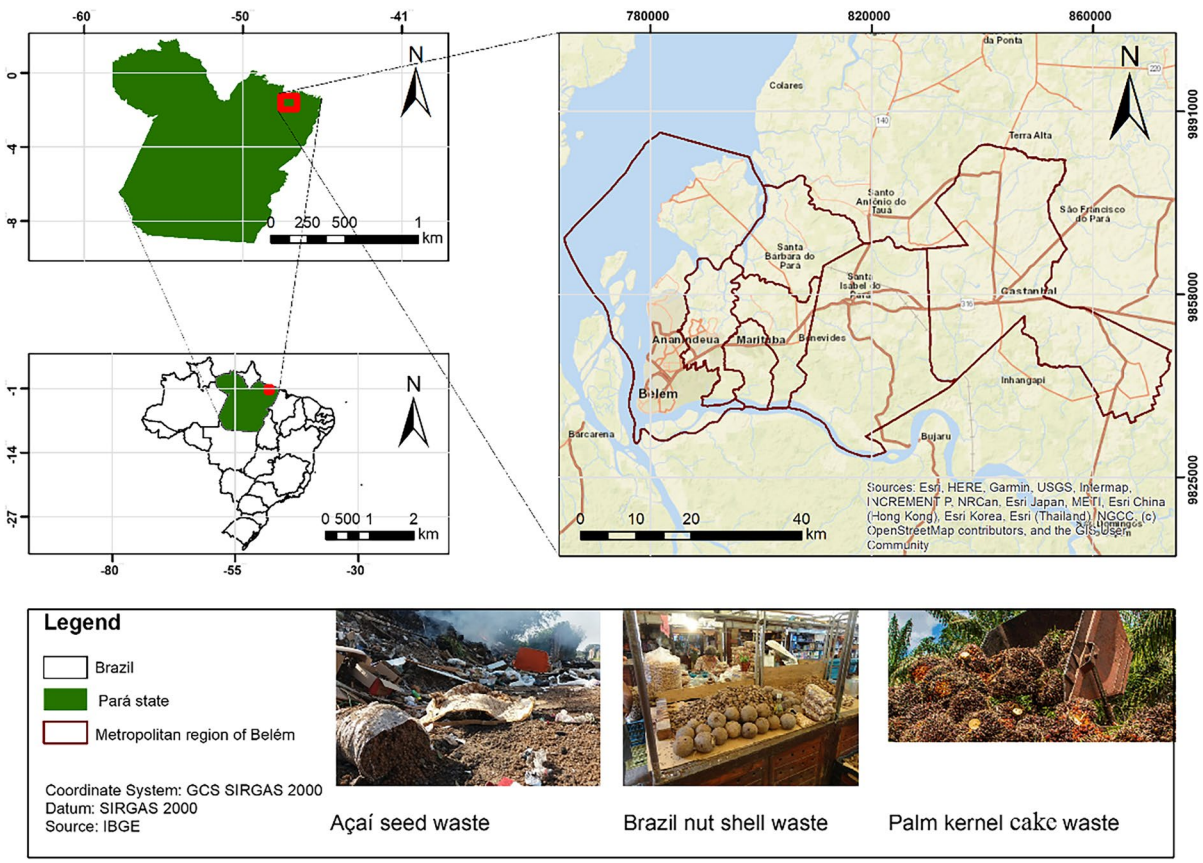

Fig. 1 Map of the acquisition location of the agro-industrial residues used for the production of biochar in this study, with emphasis on the inadequate disposal after processing of: a) açaí seeds; b) Brazil nut shell; and c) palm kernel cake

Then, 100 g of each biomass was added in ceramic crucibles with a lid to limit oxygen conditions and pyrolyzed in a muffle furnace, and subjected to a temperature of 700 ºC, under a heating rate of 3.33 ºC min^{-1} (best results of preliminary tests for physical and chemical characterization of biochars (Yuan et al., 2011).

The yield of biochars was calculated from the difference between the mass of the initial feedstock (dry material) and pyrolyzed material. The pH in water and electrical conductivity were determined by the ratio of 1:10 (solid: solution) (Singh et al., 2017). The cation exchange capacity (CEC) of the biochars was quantified by the modified NH_4 acetate displacement method (Yuan et al., 2011). The point of zero charge (PZC) was determined according to Yang et al. (2004).

The total contents of carbon (C), hydrogen (H), nitrogen (N) and sulfur (S) were determined by the PerkinElmer elemental analyzer (model 2400), using 2 mg of biochar. The percentage of oxygen was estimated by Eq. (1):

$$O\% = 100 - (ash + C + H + N + S) \quad (1)$$

The H/C, O/C and (O + N)/C atomic ratios were calculated to evaluate the aromaticity and estimate the stability of the different biochars. The P content was calculated using the EPA (3050B) method (Zhao et al., 2013). Ash content was determined by combustion of 1 g of biochar in a muffle furnace, maintained at 500 °C for 1 h, then at 750 °C for 2 h (Melo et al., 2013). Ash contents were determined according to Eq. (2). Volatile contents were calculated by the methodology by ASTM D3175-07 (Eq. 3 and 4). For more information about the characterization and results, we recommend reading the full study by Dias et al. (2019).

$$\text{Ash } (\%W) = \left(\frac{a - b}{c}\right).100 \quad (2)$$

where: a is the weight of capsule and ash residue (g); b is the weight of empty capsule and lid (g); c is the weight of sample used (g).

$$\text{Mass loss}(\%C) = (A - B).100 \quad (3)$$

where: A is the dry weight at 100 ºC (g); B is the weight of biochar after 950 ºC (g).

$$\text{Volatile material } (\%VM) = \%C - \%D \quad (4)$$

where: %C is the mass loss; and %D is the humidity.

2.3 Phosphorus Adsorption Experiment

Adsorption tests were performed to determine the maximum adsorption capacity of P on different types of biochars. For this, 0.1 g of each biochar sample was added to 30 mL of KH_2PO_4 solution in ultrapure water, with seven different concentrations of P (10, 50, 100, 150, 200, 250, 300 mg L^{-1}) at pH 8. These samples were kept under stirring on a shaking table at 130 rpm (26 °C ± 2 °C) for 13 h and filtered through a 0.45 µm filter (best results of preliminary tests). The concentration of P was determined by the molybdenum blue method (Braga & Defelipo, 1974) in UV – VIS Spectrophotometer. The maximum P adsorption capacity was obtained by means of the Langmuir isotherm described in Eq. (5).

$$q_e = \frac{q_m K_L C_e}{1 + K_L C_e} \quad (5)$$

where: q_e is the amount of adsorbed solute at equilibrium per gram of adsorbent (mg g^{-1}), C_e is the solute concentration at equilibrium (mg L^{-1}), q_m (mg g^{-1}) is the maximum adsorption capacity and K_L is the Langmuir constant.

2.4 Data Processing and Analysis

Initially, the data were evaluated by means of descriptive analysis and multivariate outliers were determined. Before conducting the multivariate statistical analyses, we verified the assumptions of normality of the residues and homogeneity of variances using the Shapiro–Wilk test and the Levene's test, respectively, both at the 5% level of significance (p-value > 0.05). Then, multivariate statistical tests were conducted, including: factor analysis (FA), canonical correlation analysis (CCA), and hierarchical clustering analyses. These analyzes aimed to reduce the number of variables and improve the understanding of which biochar properties best interact with the P adsorption process.

The FA was employed to understand the relationship of the characteristics of the biochars with the adsorption capacity of P. The first two factors were considered, with eigenvalues greater than unity (Kaiser, 1958). The coefficients of the linear functions, which define the factor loadings, were used in the interpretation of their meaning, considering the sign and the relative size of the loadings as an

indication of the weight to be attributed to each variable.

The CCA was applied to identify and quantify associations between two distinct groups of variables, generating scores for the first two canonical variables that explain the maximum possible variation (Cruz & Regazzi, 1994). The study of these associations occurs through canonical variables, from linear combinations between two groups of variables (U and V). In this study, group 1 (U; Eq. 6) was composed of the variables q_m and P content; and group 2 (V; Eq. 7) corresponded to the physicochemical properties and elemental composition of the biochars, including yield, CEC, PZC, ash, pH, C and N. In this analysis, the variables EC, VM, H, O, S, H/C, O/C, and (O + N)/C were not selected because they did not meet the principle of orthogonality with each other.

$$U = \mathbf{a}^T X^{(1)} \quad (6)$$

$$V = \mathbf{b}^T X^{(2)} \quad (7)$$

where **a** and **b** are non-zero vectors of the coefficients of these linear combinations, selected in order to maximize the correlation between the variables. Thus, this analysis makes it possible to evaluate the interrelationships between physicochemical properties and elemental composition (V) with the P adsorption process (U). The data were standardized to present mean 0 and variance 1.

Heatmaps were generated using the Euclidean distance method and employed to discriminate the biochar, as well as its characteristics that most closely resembled or contrasted with each other and with P adsorption. All statistical analyses were processed in R environment (R Core Team, 2022).

3 Results and Discussion

3.1 Multivariate Analysis

3.1.1 Factor Analysis (FA)

Two processes (factors) were identified for BA, BN and BK, which in turn explained approximately 95% of the total variability observed in the original data for the biochars (Fig. 2; Table S1). These results are consistent with the criteria by Sneath and Sokal (1973), who establish that the sum of the factors must explain at least 70% of the total variance. Factor 1 for BA represents almost 50% of the total variance observed, and considering the order of relevance of factor loadings, the following attributes were retained: PZC (-0.99), H (-0.99), O (0.99), q_m (-0.98), CEC (0.86), S (-0.85), ash (-0.82), EC (-0.79) and N (0.78) (Fig. 3; Table S1). Factor 2 for BA explained 46% of the total variability and, following the order of importance, the properties with the highest factor loadings were: O/C (-0.97), yield (0.94), P (0.92), pH (0.91), VM (0.91), (O + N/C) (-0.90), H/C (-0.87) and C (0.75) (Fig. 3; Table S1). These factor loadings represent the correlation of each variable with the factor; therefore, the higher their absolute values, the greater the relevance in interpreting the factor matrix (Hair et al., 2005).

Similarly, factor 1 explained the greatest total variance of the groups of variables for BN (55%) and BK (65%) (Fig. 2), with the variables with the highest factor loadings belonging to P content, PZC, EC, H, O, S, and atomic ratios (Fig. 3; Table S1). In turn, factor 2 was responsible for the explanation of 40% and 29% for BN and BK, respectively, and the variables that most influenced this process when we evaluate both biochars were: yield and C content.

The properties ash, CEC and N content of all biochars showed high association with q_m, both for BA and BK (factor 1) and BN (factor 2). This result suggests that, when these biochars are evaluated together, these characteristics are the mainly responsible for the variations in P adsorption rates, regardless of the raw material used, at the temperature of 700 ºC (Fig. 3). Thus, pyrolysis conditions with high temperatures, as in our study (700 ºC), lead to greater formation of ash, which in turn is linked with the preservation of inorganic compounds present in biomass, such as Ca^{2+}, Mg^{2+}, Si, K^+, and P (Wang & Liu, 2017). These elements are not degraded at high temperatures, being only transformed into oxides, hydroxides and carbonates, and remain as constituents in the material (Zhang et al., 2017).

The variable q_m showed direct association with CEC for BN (0.96) and BK (0.99) and inverse for BA (0.86) (Fig. 3). The increase in CEC is related to the higher presence of basic cations and alkalinity conditions. With that, alkalinity enables deprotonation of the active sites of functional groups and ion exchange between some elements and the basic cations (Li

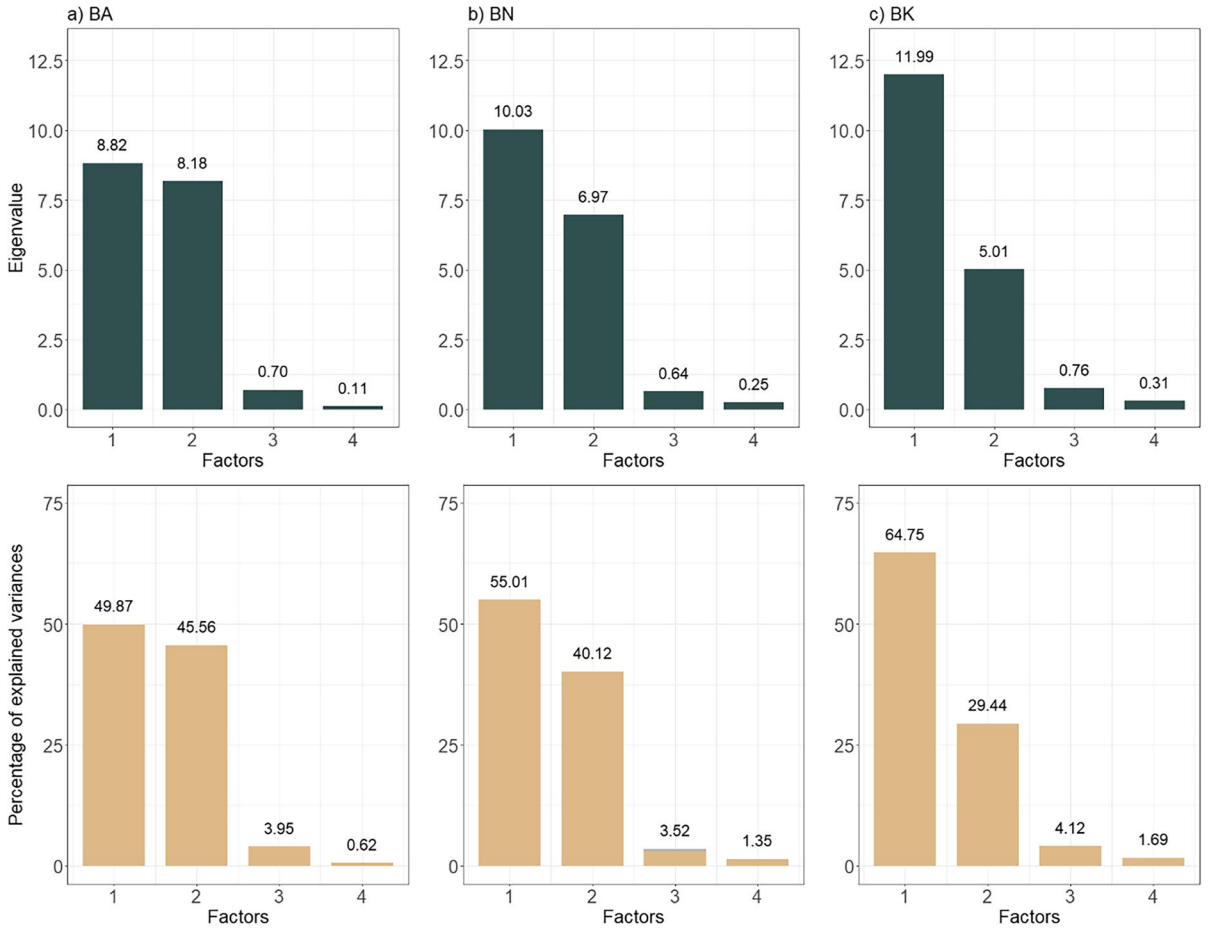

Fig. 2 Eigenvalues that are higher than the unity, used for interpretation of results and percentage of explained variances of different biochars for the four main factors of a) BA, b) BN and c) BK

et al., 2017). The opposite effect is found in acidic conditions, where ion repulsion occurs due to the presence of positive charges and competition with H^+ ions for adsorption on the biochar surface (Zhou et al., 2017). Another property strongly related to P adsorption was N content, which showed inverse association with BA (0.78) and BN (-0.99), and direct association with BK (0.99). This behavior probably results from the nature of the material used for biochar production, as BA and BN are derived from woody materials. Wang and Liu (2017) reported that biochars originated from woody materials generally have lower N content compared to biochars synthesized from agricultural residues and show promising results when used for phosphate adsorption. Thus, considering the high association between the variables q_m (0.99) and N content (0.99) for BK, we can infer that the higher the N content in the biochar, the higher the P adsorption capacity; therefore, the high N content in BK suggests higher potential of this biochar to immobilize P in soil (Chowdhury et al., 2016).

Overall, for all the biochars in this study, the elemental composition (C, H, O, N and S) showed strong direct or inverse association with P adsorption (Fig. 3; Table S1). One of the reasons for this behavior is probably linked to the pyrolysis conditions, as we used 700 ºC for the synthesis of the biochars and several studies revealed that high temperature conditions, besides promoting the adsorption of organic and inorganic compounds (Dai et al., 2020), favor a gradual loss of hydroxyls (OH) due to dehydration reactions and, consequently, release O and H to the C atoms in the original material (Li & Chen, 2018). As a consequence, there is an aromatic structure with

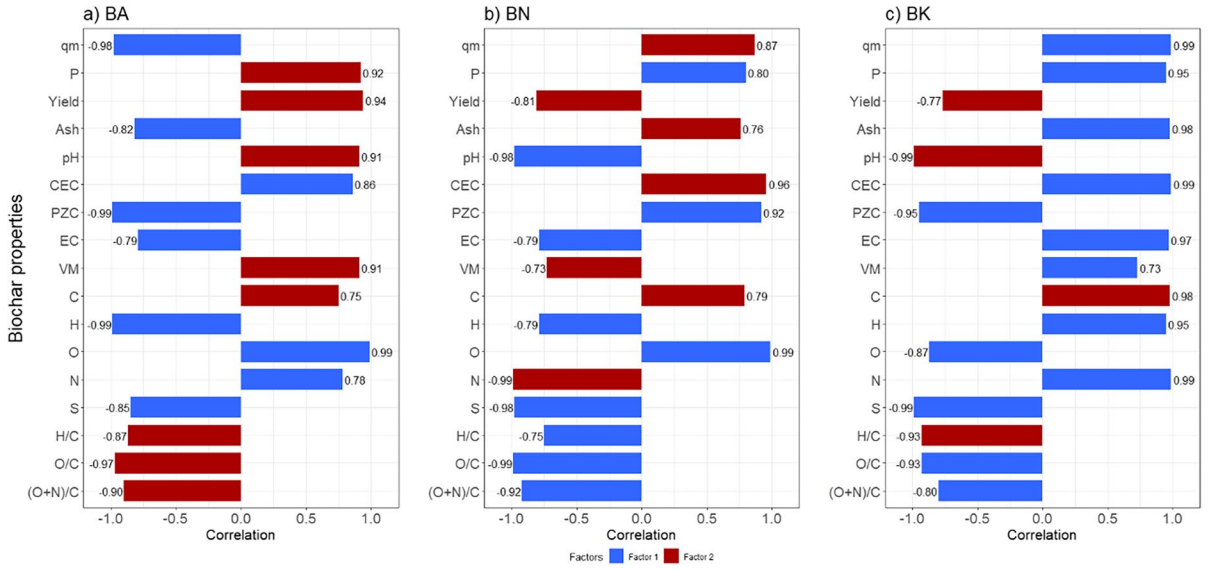

Fig. 3 Factor Analysis (FA) indicating the linear correlation coefficients between physicochemical characteristics, elemental composition and atomic ratios of different biochars for the two main factors of a) BA, b) BN and c) BK. The values shown refer to the significant factor loadings ($p < 0.05$) retained in factors 1 and 2 for the açaí seed (BA), Brazil nut shell (BN) and palm kernel cake (BK) biochars. q_m: maximum phosphorus adsorption capacity; P: phosphorus content; Ash: ash content; CEC: cation exchange capacity; PZC: point of zero charge; EC: electrical conductivity; VM: volatile material; H/C and O/C: aromaticity indices; (O + N)/C: polarity index

high thermochemical recalcitrance, which in turn provides greater stability to the biochar and thus greater potential for soil C sequestration (Sato et al., 2019).

Such findings reinforce that the type of feedstock coupled with the pyrolysis conditions (heating rate, reaction time, and pyrolysis temperature) are the main factors that determine the characteristics of biochars (Yu et al., 2017; Zhang et al., 2021). For example, biochars derived from plant residues, such as rice straw, sugarcane bagasse, and corn stalk, have a large number of elements, such as C, H, O, N, S, P, Ca, and Mg (Lu et al., 2013). In contrast to plant sources, biochars produced from urban sewage sludge at the same temperatures (300 °C) have lower contents of these elements and organic matter (OM) (Lu et al., 2013). Moreover, the pH of biochars prepared at temperatures below 450 ºC ranges from 6.6 to 10.7; and when the temperature is higher than 450 ºC, the pH is greater than 7 and therefore alkaline (Hossain et al., 2011). In this context, such characteristics should be contemplated when designing the use of biochar for specific environmental and agricultural contexts, as they allow investigating the potential use of a given biomass for specific purposes, including soil conditioning (Tan et al., 2017), soil carbon sequestration (Colantoni et al., 2016), or adsorption of organic and inorganic soil and water contaminants (Dai et al., 2020; Tan et al., 2022).

3.2 Canonical Correlation Analysis (CCA)

The canonical correlations for the pairs of variables of BA (0.962; 0.787), BN (0.941; 0.679) and BK (0.938; 0.589) and canonical R^2 for BA (0.925; 0.619), BN (0.885; 0.461) and BK (0.880; 0.347) were shown to be significant ($p < 0.01$). Because of the significance of the correlations presented, it can be concluded that the selected groups are not independent, that is, the cause-and-effect relationships that occur in one group are closely linked to the other group (Table 1). This means that the adsorption of P represented by the first group of variables (U1) and the physicochemical characteristics and elemental composition (V1) are coupled processes and occur simultaneously in the biochars.

Table 2 shows the correlations between the variables of the canonical component that represents them (U_k and V_k), called canonical loadings, as well as the

Table 1 Eigenvalues and canonical correlations for the phosphorus dynamics and physicochemical variables and elemental composition of BA, BN and BK.

Pairs of canonical variables[a]		Canonical correlation	Canonical R^2 (eigenvalues)	χ^2	DF[b]	p-value[c]
BA	(U1, V1)	0.962	0.925	385.36	14	$<0.001^{**}$
	(U2, V2)	0.787	0.619	164.06	6	$<0.001^{**}$
BN	(U1, V1)	0.941	0.885	367.52	14	$<0.001^{**}$
	(U2, V2)	0.679	0.461	154.66	6	$<0.001^{**}$
BK	(U1, V1)	0.938	0.880	362.48	14	$<0.001^{**}$
	(U2, V2)	0.589	0.347	153.22	6	$<0.001^{**}$

[a]U_n = canonical variables for P adsorption related attributes of the biochars, V_n = canonical variables for physicochemical attributes and elemental composition of the biochars. [b]degree of freedom. [c**]significant at 1% probability level

correlations of these variables with another canonical component, known as cross canonical loadings. Such values help in the understanding of canonical variables, because the higher the absolute value of a canonical loading, the greater the association between the original variable and its respective canonical component. It was observed that the total proportions explained separately by the properties linked to P adsorption (U1) were 66.58% (BA), 64.30% (BN) and 64.22% (BK). On the other hand, the variables related to physicochemical characteristics and elemental composition (V1) separately explained 46.64% (BA), 37.12% (BN) and 36.85% (BK) of the total variation in this group. The canonical variable U1 for BA showed the highest values in modulus of the canonical correlation for P content (-0.95) when compared to the other variable in the same group q_m (0.58). Conversely, q_m presented the highest canonical loading (0.82) in U2 for BA. Therefore, these results indicate that U1 is mainly related to the P content and U2 can be described as the P adsorption phenomenon.

High canonical cross-loadings were obtained between P adsorption and chemical attributes of BA (U2), mainly PZC (0.97), pH (0.78) and contents of ash (0.98) and C (0.93) (Table 2). These variables present positive and direct association with q_m; thus, we can infer that higher increments in these attributes can condition higher adsorption for BA. Unlike BA, the canonical variable q_m (U1) presented the highest values in modulus for BN (0.93) and BK (0.88) (Table 2). Thus, we can assume that for these biochars U1 is predominantly linked to P adsorption processes. The high canonical cross-loadings in U1 indicate that the properties that most influenced this process for BN were CEC (0.96), ash content (0.99) and N content (-0.93); and for BK the main properties were yield (-0.83), CEC (-0.99), PZC (-0.92), ash content (0.95) and N content (0.98).

The redundancy index (RI) expresses the amount of variance in a canonical statistical variable (dependent or independent) explained by the other canonical statistical variable. In this study, RI indicates that 86.25%, 84.93% and 84.36% of the total variation of the P adsorption process can be described as a function of the variation in physicochemical attributes and elemental composition for BA, BN and BK, respectively, in the first canonical correlation (Table 2). On the other hand, only 13.75%, 15.07% and 15.64% of the total variation in physicochemical attributes and elemental composition were explained by P adsorption in the first canonical correlation. These results support the understanding that the P adsorption process depends on the properties of the biochars, mainly PZC and ash content for BA and CEC, ash and N for BN and BK.

3.3 Hierarchical Cluster Analysis

The heatmap plot using multivariate cluster analysis and Euclidean distance as the method of metric distance between the groups (Fig. 4) indicated the presence of three clusters (groups I, II and III) significant with the distinction between the properties of biochars. In addition, the color scale on the heatmap evidenced in which biochar the studied characteristics are more or less expressive (Fig. 4).

The results of Fig. 4 suggest that group I, formed by the properties q_m, pH, C content, CEC, S and EC, has more similarity among themselves when compared to groups II (H/C, VM, O, H, yield, and PZC) and III (O/C, (O + N)/C, ash, N and P). Groups II and III, among other attributes, are formed by characteristics

Table 2 Correlation between physicochemical variables and elemental composition of BA, BN and BK, based on canonical correlation analysis (CCA)

Variable	Canonical loadings		Cross canonical loadings		Canonical loadings		Cross canonical loadings		Canonical loadings		Cross canonical loadings	
	BA				BN				BK			
	U1	U2	V1	V2	U1	U2	V1	V2	U1	U2	V1	V2
q_m	0.58	0.82	0.62	0.74	0.93	0.28	0.88	0.08	0.88	-0.25	0.81	-0.36
P	-0.95	0.20	-0.86	0.34	-0.84	0.54	-0.82	0.46	0.76	-0.47	0.79	-0.33
PVE (%)	66.58	33.42	-	-	64.30	35.70	-	-	64.22	35.78	-	-
RI (%)	86.25	-	-	-	84.93	-	-	-	84.36	-	-	-
	Canonical loadings		Cross canonical loadings		Canonical loadings		Cross canonical loadings		Canonical loadings		Cross canonical loadings	
	V1	V2	U1	U2	V1	V2	U1	U2	V1	V2	U1	U2
Yield	-0.71	0.67	-0.76	0.69	-0.36	-0.65	-0.39	-0.67	-0.75	-0.58	-0.83	-0.62
CEC	-0.80	-0.60	-0.84	-0.65	0.93	0.24	0.96	0.27	0.97	-0.05	0.99	-0.12
PZC	0.28	0.96	0.36	0.97	-0.18	0.70	-0.26	0.72	-0.89	0.44	-0.92	0.47
Ash	-0.17	0.97	-0.24	0.98	0.97	0.01	0.99	0.12	0.93	-0.37	0.95	-0.42
pH	-0.64	0.74	-0.69	0.78	0.58	-0.49	0.63	-0.53	-0.30	-0.88	-0.37	-0.90
C	-0.41	0.89	-0.44	0.93	0.32	0.66	0.37	0.68	0.36	0.86	0.39	0.88
N	-0.88	-0.47	-0.92	-0.54	-0.90	-0.32	-0.93	-0.39	0.96	-0.08	0.98	-0.18
PVE (%)	46.64	28.37	-	-	37.12	24.96	-	-	36.85	23.34	-	-
RI (%)	13.75	-	-	-	15.07	-	-	-	15.64	-	-	-

q_m Maximum phosphorus adsorption capacity; *P* Phosphorus content; *CEC* Cation exchange capacity; *PZC* Point of zero charge; *Ash* Ash content; *pH* Hydrogen potential; *C* Carbon content; *N* Nitrogen content; *PVE (%)* Proportion of variation explained; *RI* Redundancy index

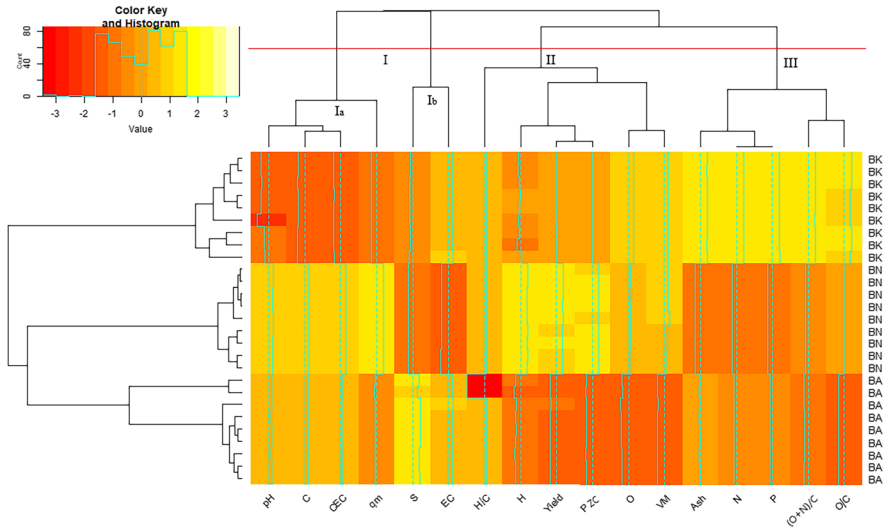

Fig. 4 Heatmap plot with physicochemical properties, elemental composition and atomic ratios for biochars synthesized from açaí seed residue (BA), Brazil nut shell (BN) and palm kernel cake (BK). The heatmap shows the variations in the characteristics of the biochars as a function of the feedstock used. The dendrogram above the heatmap represents the grouping of the biochars based on similar patterns of variation. q_m: maximum phosphorus adsorption capacity; Ash: ash content; CEC: cation exchange capacity; PZC: point of zero charge; EC: electrical conductivity; VM: volatile material; H/C and O/C: aromaticity indices; (O + N)/C: polarity index

associated with atomic ratios, such as the aromaticity indices H/C and O/C; and the polarity index (O + N)/C. Studies show that the aromatic content confers high chemical stability and resistance of biochar to chemical and microbial degradation, contributing to the persistence of these materials in soils (Ullah et al., 2019). While this characteristic is desirable in terms of effective and long-lasting environmental remediation, carbon sequestration, and supporting global greenhouse gas (GHG) mitigation actions (Colantoni et al., 2016), the aromatic structure shows less polarity compared to the aliphatic and therefore less surface charge (Uchimiya et al., 2011), which in turn hinders the adsorption process.

The aromaticity ratio O/C is the property most distant from q_m (Fig. 4), indicating that these properties exhibit the most contrasting behavior. The O/C ratio provides an additional indication of the pyrolysis conditions (Carnevale et al., 2022). For example, O/C values > 0.7 indicate that there was a predominance of oxidizing conditions in the pyrolysis, resulting in a low-quality biochar (Conte et al., 2015). Corroborating with this observation, Chatterjee et al. (2020) reported that the decrease in O/C ratio in biochar synthesized at high temperatures from agro-industrial residue, reflects the increasing carbonization rate and consequent increase in C content and the decrease in O content, which is probably linked to the breakdown of oxygenated bonds and release of low molecular weight by-products containing H and O. In addition, this property may be an index of polar groups, as higher O/C values indicate hydrophilicity (affinity of the material with water), while lower O/C ratios suggest hydrophobic character (repelling of the biochar to water) (Carnevale et al., 2022).

The O/C atomic ratios found for this study were low for all biochars (Table S2), especially for the woody materials BA (0.14) and BN (0.18) compared to BK (0.23). According to Spokas (2010), the O/C ratio is an indication of weathering (oxidation) of the biochar as well as other black C literature that correlate O/C to black C properties and stability. This author proposed that the highest stability for biochars can be described as a function of the lowest O/C ratio. To this end, based on the O/C value, this author defined three groups of biochars by predicting the half-life of the biochar, namely: i) O/C ≥ 0.6 (half-life ≤ 100 years), ii) 0.2 ≥ O/C ≤ 0.6 (1000-year half-life > 100 years) and iii) O/C < 0.2 (half-life > 1000 years). Therefore, this indicates

that BA and BN are the most recalcitrant materials, possessing an estimated half-life of more than 1000 years. Biochars characterized with a O/C < 0.4 and H/C < 0.6 are suggested as promising technologies for carbon sequestration (Ippolito et al., 2012). In this perspective, our results indicate that the three biochars produced in this study have potential for application as carbon sequestration agents. Other studies have also used the O/C ratio as the biochar stability indicator (Bong et al., 2022; Choi et al., 2017; Crombie et al., 2013).

The H/C ratio is an indicator of the carbonization degree of the material. The lower this ratio, the greater the degree of polycondensation and permanence of the material in the environment (Conte et al., 2015). The very low H/C ratios found for the biochars (Table S2) suggest that C in these materials is predominantly unsaturated, so that most of the C atoms are directly bound to other C (Usevičiūtė & Baltrėnaitė-Gedienė, 2020). Moreover, considering that C content, pH, and q_m were arranged in the same group and show a similar color gradient (Fig. 4), we can infer that there is a direct association between these variables. The pH plays an important role in adsorption mechanisms and is closely linked in determining the distribution of phosphate between the fast and slow-release components (Xu et al., 2022). This characteristic is very useful when biochar is used to supply phosphate in agricultural environments, because the fast-release components relate to the supply of phosphate needed for plant establishment, while the slow-release compounds are used to ensure a constant supply of phosphate for longer periods (Arbelaez Breton et al., 2021). Schneider and Haderlein (2016) reported that labile organic carbon from biochars produced at low pyrolysis temperatures can inhibit P adsorption in tropical soils, which predominantly contain iron (Fe) and aluminum (Al) oxides. For example, in low-temperature (<450 °C) pyrolyzed biochars, labile organic carbon fractions and higher presence of functional groups predominate, which may reduce P sorption due to competitive reactions between P and various types of low molecular weight organic acids and anions (Ghodszad et al., 2022; Schneider & Haderlein, 2016).

3.4 Environmental and Agricultural Management

Tropical regions generally present soils with a higher degree of weathering due to the higher rainfall regime and high temperatures (Sato et al., 2019). In intensely weathered soils, kaolinite, iron and aluminum oxides predominate in the clay fraction, which results in low CEC, low macronutrient availability and high dependence on organic C content (Domingues et al., 2017). In addition, there is a low P concentration and a high adsorption capacity since deficiency results in crop yield reduction (Gollany et al., 2015). In this case, the application of biochar from agro-industrial residue, produced at 700 ºC, enriched with P, can be a strategy to increase soil pH, pH-dependent negative charges (Domingues et al., 2020) and constitute a phosphate biofertilizer. This effect can replace or complement the large amounts of limestone used to correct soil acidity in agricultural areas (Domingues et al., 2017) and optimize the use of phosphate fertilizers.

Properties such as C content and the aromaticity and hydrophobicity indices can be used as predictor covariates of chemical stability and consequent persistence of biochar in soils. At elevated temperatures, high C content and low H/C and O/C ratios are key indicators of aromatic character, stability against degradation in soils, and consequently longer C residence time in biochar-treated soils. In our study, the woody biomasses BA and BN showed higher C content (79.29% and 80.22%, respectively) and O/C less than 0.20% when compared to BK (67.49% and 0.22%). With this, BA and BN are expected to show greater persistence in the environment than BK. Therefore, the use of these biochars, besides allowing the proper management of agro-industrial residues, represents a key strategy to adsorb P from the soil and increase the thermochemical stability of C in Brazilian soils.

4 Conclusion

The multivariate analysis identified the main properties of biochars that control the phosphorus adsorption process and carbon thermochemical stability. In addition, it provided the differentiation between the biochars coming from different agro-industrial residues, based on physicochemical characteristics, elemental composition and atomic ratios. Canonical correlation analysis highlighted the sensitivity of phosphorus adsorption to changes in chemical attributes and elemental composition, such as PZC, ash and C (BA); CEC, ash and N (BN); yield, ash, CEC, PZC and N (BK). Factor analysis indicated a high association between P adsorption with the properties

ash, CEC and N, indicating that small increments in these attributes can cause an increase in the rate of P adsorption. The biochars derived from woody biomasses showed greater similarities and greater contrast between the adsorption of P with the aromaticity indices H/C and O/C and the polarity index (O + N)/C. Furthermore, BA and BN showed greater chemical stability (high carbon content and lower O/C ratios) than BK. Multivariate analyses were able to capture natural correlations and multiple influences of biochar characteristics on P adsorption behavior and highlighted the heterogeneity of mineral constituents for all biochars. Thus, our results indicate that biochars derived from açaí, Brazil nut and palm kernel cake can be used as phosphate biofertilizer, increase the thermochemical stability of C in soil and represent potential alternative materials for waste management of eastern Amazon.

Author Contribution All authors contributed to the study conception, design and methodology. Material preparation, data collection, formal analysis and first draft of the manuscript were performed by **Kleve F. F. Canteral**. The review and editing were done by **Yan N. Dias** and **Antonio R. Fernandes**. All authors read and approved the final manuscript.

Data Availability The datasets generated during and/or analysed during the current study are available from the corresponding author on reasonable request.

Declarations

Ethics Declaration Statement Not applicable.

Consent to Participate Not applicable.

Consent for Publication Not applicable.

Conflict of Interests The authors declare that they have no known competing financial interests or personal.

References

ABRAPALMA - Brazilian Palm Oil Producers Association. (2019). Available In: ⟨http://www.abrapalma.org/pt/⟩. Accessed 16 September 2022.

Arbelaez Breton, L., Mahdi, Z., Pratt, C., & El Hanandeh, A. (2021). Modification of hardwood derived biochar to improve phosphorus adsorption. *Environments – MDPI*, *8*. https://doi.org/10.3390/environments8050041

Bong, H. K., Selvarajoo, A., & Arumugasamy, S. K. (2022) Stability of biochar derived from banana peel through pyrolysis as alternative source of nutrient in soil: feed-forward neural network modelling study. *Environmental Monitoring and Assessment*, *194*. https://doi.org/10.1007/s10661-021-09691-x

Braga, J. M., & Defelipo, B. V. (1974). Spectrophotometric determination of phosphorus in soil and plant extracts (Determinação espectrofotométrica de fósforo em extratos de solo e material vegetal). *Revista Ceres, 21*, 73–85.

Carnevale, M., Longo, L., Gallucci, F., et al. (2022). Influence of the harvest time and the airflow rate on the characteristics of the Arundo biochar produced in a pilot updraft reactor. *Biomass Conversion and Biorefinery*, *12*, 2525–2539. https://doi-org.ez87.periodicos.capes.gov.br/10.1007/s13399-020-01241-8

Chatterjee, R., Sajjadi, B., Chen, W. Y., Mattern, D. L., Hammer, N., Raman, V., & Dorris, A. (2020). Effect of pyrolysis temperature on physicochemical properties and acoustic-based amination of biochar for efficient CO2 adsorption. *Frontiers in Energy Research, 8*, 1–18. https://doi.org/10.3389/fenrg.2020.00085

Choi, J., Nam, H., Carter, S., & Capareda, S. C. (2017). Tuning the physicochemical properties of biochar derived from Ashe juniper by vacuum pressure and temperature. *Journal of Environmental Chemical Engineering*, *5*, 3649–3655. https://doi-org.ez87.periodicos.capes.gov.br/10.1016/j.jece.2017.07.028

Chowdhury, Z. Z., Ziaul Karim, M., Ashraf, M. A., & Khalid, K. (2016). Influence of carbonization temperature on physicochemical properties of biochar derived from slow pyrolysis of durian wood (Durio zibethinus) sawdust. *BioResources, 11*, 3356–3372. https://doi.org/10.15376/biores.11.2.3356-3372

Colantoni, A., Evic, N., Lord, R., Retschitzegger, S., Proto, A. R., Gallucci, F., & Monarca, D. (2016). Characterization of biochars produced from pyrolysis of pelletized agricultural residues. *Renewable and Sustainable Energy Reviews, 64*, 187–194. https://doi.org/10.1016/j.rser.2016.06.003

Conte, P., Schmidt, H., & Cimò, G. (2015). Research and application of biochar in Europe. *Agricultural and Environmental Applications of Biochar: Advances and Barriers*, 1–21. https://doi-org.ez87.periodicos.capes.gov.br/10.2136/sssaspecpub63.2014.0050

Crombie, K., Mašek, O., Sohi, S. P., Brownsort, P., & Cross, A. (2013). The effect of pyrolysis conditions on biochar stability as determined by three methods. *Gcb Bioenergy., 5*, 122–131. https://doi.org/10.1111/gcbb.12030

Cruz, C. D., & Regazzi, A. J. (1994). *Modelos Biométricos Aplicados Ao Melhoramento Genético*. Universidade Federal de Viçosa.

Dai, Y., Wang, W., Lu, L., Yan, L., & Yu, D. (2020). Utilization of biochar for the removal of nitrogen and phosphorus. *Journal of Cleaner Production*, *257*. https://doi.org/10.1016/j.jclepro.2020.120573

Dias, Y. N., Souza, E. S., Da Costa, H. S. C., Melo, L. C. A., Penido, E. S., Do Amarante, C. B., Teixeira, O. M. M., Fernandes, A. R. (2019) Biochar produced from Amazonian agro-industrial wastes: properties and adsorbent potential of Cd2+ and Cu2+. *Biochar*, 1, 389–400. https://doi.org/10.1007/s42773-019-00031-4

Domingues, R. R., Sánchez-Monedero, M. A., Spokas, K. A., Melo, L. C. A., Trugilho, P. F., Valenciano, M. N., & Silva, C.

A. (2020). Enhancing cation exchange capacity ofweathered soils using biochar: Feedstock, pyrolysis conditions and addition rate. *Agronomy, 10*, 1–17. https://doi.org/10.3390/agronomy10060824

Domingues, R. R., Trugilho, P. F., Silva, C. A., De Melo, I. C. N. A., Melo, L. C. A., Magriotis, Z. M., & Sánchez-Monedero, M. A. (2017). Properties of biochar derived from wood and high-nutrient biomasses with the aim of agronomic and environmental benefits. *PLoS ONE, 12*, 1–12. https://doi.org/10.1371/journal.pone.0176884

Fahmy, T. Y., Fahmy, Y., Mobarak, F., El-Sakhawy, M., Abou-Zeid, R. E. (2020). Biomass pyrolysis: past present and future. *Environment Development and Sustainability.* 22, 17–32.https://doi.org/10.1007/s10668-018-0200-5

Ghodszad, L., Reyhanitabar, A., Oustan, S., & Alidohkt, L. (2022). Phosphorus sorption and desorption characteristics of soils as affected by biochar. *Soil and Tillage Research, 216*, 105251. https://doi.org/10.1016/j.still.2021.105251

Gollany, H. T., Titus, B. D., Scott, D. A., Asbjornsen, H., Resh, S. C., Chimner, R. A., Kaczmarek, D. J., Leite, L. F. C., Ferreira, A. C. C., Rod, K. A., Hilbert, J., Galdos, M. V., & Cisz, M. E. (2015). Biogeochemical research priorities for sustainable biofuel and bioenergy feedstock production in the Americas. *Environmental Management, 56*, 1330–1355. https://doi.org/10.1007/s00267-015-0536-7

Hair, J. F., Anderson, R. E., Tatham, R. L., & Black, W. (2005). *Multivariate Data Analysis*. Prentice Hall.

Hossain, M. K., Strezov, V., Chan, K. Y., Ziolkowski, A., Nelson, P. F. (2011). Influence of pyrolysis temperature on production and nutrient properties of wastewater sludge biochar. *Journal of environmental management*, 92, 223–228.https://doi.org/10.1016/j.jenvman.2010.09.008

IBGE. (2019). Instituto Brasileiro de Geografia e Estatística - Production of Plant Extraction and Silviculture. Available In: ⟨http://www.ibge.gov.br⟩. Accessed on 9 June 2022. (In Portuguese).

IPCC. (2018). Global Warming of 1.5 °C. An IPCC Special Report on the impacts of global warming of 1.5 °C above pre-industrial levels and related global greenhouse gas emission pathways, in the context of strengthening the global response to the threat of climate change, sustainable development, and efforts to eradicate poverty. Masson-Delmotte, V., Zhai, P., Pörtner, H. -O., Roberts, D., Skea, J., Shukla, P. R., Pirani, A., Moufouma-Okia, W., Péan, C., Pidcock, R., Connors, S., Matthews, J. B. R., Chen, Y., Zhou, X., Gomis, M. I., Lonnoy, E., Maycock, T., Tignor, M., & Waterfield, T. (Eds.).

Ippolito, J. A., Laird, D. A., & Busscher, W. J. (2012). Environmental benefits of biochar. *Journal of Environmental Quality, 41*, 967–972. https://doi.org/10.2134/jeq2012.0151

Kaiser, H. F. (1958). The varimax criterion for analytic rotation in factor analysis. *Psychometrika, Urbana, 23*(3), 187–200.

Lehmann, J., & Joseph, S. (2009). Biochar for environmental management: an introduction. *Biochar for environmental management: science and technology* (405). Earthscan.

Li, H., Dong, X., da Silva, E. B., de Oliveira, L. M., Chen, Y., & Ma, L. Q. (2017). Mechanisms of metal sorption by biochars: Biochar characteristics and modifications. *Chemosphere, 178*, 466–478. https://doi.org/10.1016/j.chemosphere.2017.03.072

Li, S., & Chen, G. (2018). Thermogravimetric, thermochemical, and infrared spectral characterization of feedstocks and biochar derived at different pyrolysis temperatures. *Waste Management, 78*, 198–207. https://doi.org/10.1016/j.wasman.2018.05.048

Lu, H., Zhang, W., Wang, S., Zhuang, L., Yang, Y., & Qiu, R. (2013). Characterization of sewage sludge-derived biochars from different feedstocks and pyrolysis temperatures. *Journal of Analytical and Applied Pyrolysis, 102*, 137–143. https://doi.org/10.1016/j.jaap.2013.03.004

Melo, L. C. A., Coscione, A. R., Abreu, C. A., Puga, A. P., & Camargo, O. A. (2013). Influence of pyrolysis temperature on cadmium and zinc sorption capacity of sugar cane straw-derived biochar. *BioResources, 8*, 4992–5004. https://doi.org/10.15376/biores.8.4.4992-5004

R Development Core Team. (2022). A Language and Environment for Statistical Computing. R Foundation for Statistical Computing, Vienna, Austria.

Reitzel, K., Bennett, W. W., Berger, N., Brownlie, W. J., Bruun, S., Christensen, M. L., Cordell, D., Van Dijk, K., Egemose, S., Eigner, H., Glud, R. N., Grönfors, O., Hermann, L., Houot, S., Hupfer, M., Jacobs, B., Korving, L., Kjærgaard, C., Liimatainen, H., … Metson, G. S. (2019). New training to meet the global phosphorus challenge. *Environmental Science and Technology, 53*, 8479–8481. https://doi.org/10.1021/acs.est.9b03519

Sato, M. K., de Lima, H. V., Costa, A. N., Rodrigues, S., Pedroso, A. J. S., & de Freitas Maia, C. M. B. (2019). Biochar from Acai agroindustry waste: Study of pyrolysis conditions. *Waste Management, 96*, 158–167. https://doi.org/10.1016/j.wasman.2019.07.022

Schneider, F., & Haderlein, S. B. (2016). Potential effects of biochar on the availability of phosphorus - mechanistic insights. *Geoderma, 277*, 83–90. https://doi.org/10.1016/j.geoderma.2016.05.007

Singh, B., Camps-Arbestain, M., Lehmann, J., & CSIRO (Australia),. (2017). *Biochar: A guide to analytical methods*. CSIRO Publishing.

Sneath, P. H. A., & Sokal, R. R. (1973). *Numerical taxonomy: The principles and practice of numerical classification*. Freeman.

Spokas, K. A. (2010). Review of the stability of biochar in soils: Predictability of O: C molar ratios. *Carbon Management, 1*, 289–303. https://doi.org/10.4155/cmt.10.32

Tan, S. Y., Sethupathi, S., Leong, K. H., & Ahmad, T. (2022). Mechanism and kinetics of low concentration total phosphorus and reactive phosphate recovery from aquaculture wastewater via calcined eggshells. *Water, Air, & Soil Pollution, 233*, 445. https://doi.org/10.1007/s11270-022-05905-1

Tan, Z., Lin, C. S. K., Ji, X., & Rainey, T. J. (2017). Returning biochar to fields: A review. *Applied Soil Ecology, 116*, 1–11. https://doi.org/10.1016/j.apsoil.2017.03.017

Uchimiya, M., Klasson, K. T., Wartelle, L. H., & Lima, I. M. (2011). Influence of soil properties on heavy metal sequestration by biochar amendment: 1. Copper sorption isotherms and the release of cations. *Chemosphere., 82*, 1431–1437. https://doi.org/10.1016/j.chemosphere.2010.11.050

Ullah, H., Abbas, Q., Ali, M. U., Cheema, A. I., Yousaf, B., & Rinklebe, J. (2019). Synergistic effects of low-/medium-vacuum carbonization on physico-chemical properties and stability characteristics of biochars. *Chemical Engineering Journal*, *373*, 44–57. https://doi-org.ez87.periodicos.capes.gov.br/10.1016/j.cej.2019.05.025

Usevičiūtė, L., & Baltrėnaitė-Gedienė, E. (2020). Dependence of pyrolysis temperature and lignocellulosic physical-chemical properties of biochar on its wettability. *Biomass Conversion and Biorefinery*. https://doi.org/10.1007/s13399-020-00711-3

Wang, Y., & Liu, R. (2017). Comparison of characteristics of twenty-one types of biochar and their ability to remove multi-heavy metals and methylene blue in solution. *Fuel Processing Technology, 160*, 55–63. https://doi.org/10.1016/j.fuproc.2017.02.019

Xu, M., Gao, P., Yang, Z., Su, L., Wu, J., Yang, G., Zhang, X., Ma, J., Peng, H., & Xiao, Y. (2019). Biochar impacts on phosphorus cycling in rice ecosystem. *Chemosphere, 225*, 311–319. https://doi.org/10.1016/j.chemosphere.2019.03.069

Xu, S., Zhu, S., & Xiong, H. (2022). phosphate adsorption removals by five synthesized isomeric α-, β-, γ-FeOOH. *Water, Air, & Soil Pollution, 233*, 454. https://doi.org/10.1007/s11270-022-05916-y

Yang, Y., Chun, Y., Shang, G., & Huang, M. (2004). pH-dependence of pesticide adsorption by wheat-residue-derived black carbon. *Langmuir, 20*, 6736–6741. https://doi.org/10.1021/la049363t

Yu, K. L., Lau, B. F., Show, P. L., Ong, H. C., Ling, T. C., Chen, W. H., Ng, E. P., & Chang, J. S. (2017). Recent developments on algal biochar production and characterization. *Bioresource Technology, 246*, 2–11. https://doi.org/10.1016/j.biortech.2017.08.009

Yuan, J. H., Xu, R. K., & Zhang, H. (2011). The forms of alkalis in the biochar produced from crop residues at different temperatures. *Bioresource Technology, 102*, 3488–3497. https://doi.org/10.1016/j.biortech.2010.11.018

Zhang, H., Liu, Z., & Liu, S. (2016). HMGB1 induced inflammatory effect is blocked by CRISPLD2 via MiR155 in hepatic fibrogenesis. *Molecular Immunology, 69*, 1–6. https://doi.org/10.1016/j.molimm.2015.10.018

Zhang, T., Zhu, X., Shi, L., Li, J., Li, S., Lü, J., & Li, Y. (2017). Efficient removal of lead from solution by celery-derived biochars rich in alkaline minerals. *Bioresource Technology, 235*, 185–192. https://doi.org/10.1016/j.biortech.2017.03.109

Zhang, Y., Wang, J., & Feng, Y. (2021). The effects of biochar addition on soil physicochemical properties: A review. *Catena, 202*, 105284. https://doi.org/10.1016/j.catena.2021.105284

Zhao, L., Cao, X., Mašek, O., & Zimmerman, A. (2013). Heterogeneity of biochar properties as a function of feedstock sources and production temperatures. *Journal of Hazardous Materials, 256–257*, 1–9. https://doi.org/10.1016/j.jhazmat.2013.04.015

Zhou, Y., Liu, X., Xiang, Y., Wang, P., Zhang, J., Zhang, F., Wei, J., Luo, L., Lei, M., & Tang, L. (2017). Modification of biochar derived from sawdust and its application in removal of tetracycline and copper from aqueous solution: Adsorption mechanism and modelling. *Bioresource Technology, 245*, 266–273. https://doi.org/10.1016/j.biortech.2017.08.178